THE JOURNAL OF PHYSICAL CHEMISTRY B

Article

pubs.acs.org/JPCB

Three-Dimensional Ordered Macroporous (3DOM) Composite for Electrochemical Study on Acetylcholinesterase Inhibition Induced by Endogenous Neurotoxin

Yingqiao Teng,[†] Ying Fu,[†] Lili Xu,[†] Bin Lin,[†] Zhongchuan Wang,[‡] Zhiai Xu,[†] Litong Jin,[†] and Wen Zhang*[,†]

[†]Department of Chemistry, East China Normal University, Shanghai 200062, P. R. China

[‡]Department of Anorectal Surgery, Xinhua Hospital, Affiliated to School of Medicine of Shanghai Jiaotong University, Shanghai 200092, P. R. China

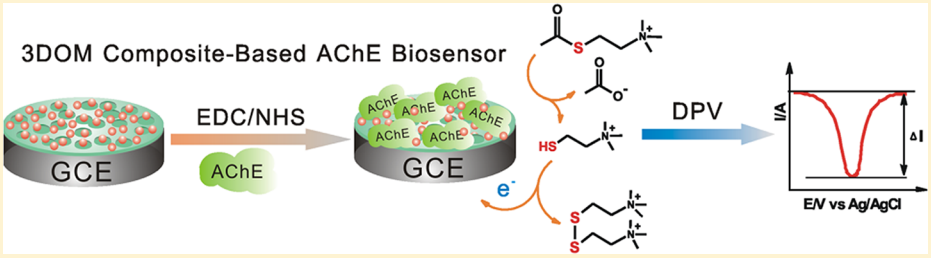

ABSTRACT: In this paper, an electrochemical acetylcholinesterase (AChE) inhibition assay based on three-dimensional ordered macroporous (3DOM) composite was conducted. The 3DOM composite was first fabricated on the glassy carbon electrode by electropolymerization of aniline in the presence of ionic liquid (IL) on a sacrificial silica nanospheres template. After the silica nanospheres were etched, an IL-doped polyaniline (IL-PANI) film with 3DOM morphology was formed. Then, gold nanoparticles (AuNPs) were decorated on the IL-PANI film by electrodeposition. The immobilized AChE on the 3DOM composite displayed favorable affinity to substrate acetylthiocholine chloride (ATCh), and the 3DOM composite showed excellent electrocatalytic effect on thiocholine, the hydrolysis product of ATCh. The presence of IL and AuNPs could improve the sensitivity by accelerating the electron transfer. The designed AChE biosensor was successfully applied to evaluate the AChE inhibition induced by endogenous neurotoxin 1(*R*),2*N*-dimethyl-6,7-dihydroxy-1,2,3,4-tetrahydroisoquinoline [(*R*)-NMSal]. The results demonstrate that (*R*)-NMSal exerts a considerable effect on AChE activity, and the inhibition is reversible. The developed method offers a new approach for AChE inhibition assay, which is of great benefit in understanding the mechanism behind neurotoxin-induced neurodegenerative disorders.

INTRODUCTION

The development of the biosensor plays a vital role in therapeutics and diagnostics.[1,2] For designing a biosensor device which combines a biorecognition element with a transducer, one critical point is to choose an ideal biomolecule immobilization matrix. The matrix should provide favorable microenvironment around the biomolecule that stabilizes its biological activity, as well as large surface area for biomolecule−substrate contact within small total volume.[3−6] In this regard, nanomaterials such as nanoparticles, nanowires, nanorods, carbon nanotubes, and graphene have been widely used in biosensing with good performances.[7−13] The good performances result from the favorable properties of nanomaterials such as large surface area, tunable electron transport abilities, and biocompatibility. The other important aspect of designing biosensor is to choose the transducer. Among the various analytical methods such as photoelectrochemical detection,[14,15] colorimetry,[16] electrochemistry,[17] fluorescence,[18] and surface plasmon resonance assay,[19] electrochemical assay is a promising one due to its high sensitivity, easy operation, and compatibility for miniaturization. For electrochemical biosensor, conductivity is an important requirement. Over the past decade, conducting polymers, especially polyaniline (PANI), have been attracting immense interest in the bioelectrochemical field because of its high conductivity, simplicity of synthesis from an inexpensive monomer, and extraordinary stability in air.[20−22] However, PANI has very low conductivity and little redox activity in neutral solutions, which is required for enzyme reaction.[23,24] In order to overcome such limitations, doping it with different anions is an effective method.[25,26]

Recently, ionic liquids (ILs) have gained increasing attention in the areas of electrochemistry and biosensors.[27−38] ILs are defined as a group of organic salts consisting entirely of ions that exist in the form of a liquid at a low temperature (<100 °C). They possess unique properties such as negligible vapor pressure, wide potential windows, high thermal stability and

Received: March 23, 2012
Revised: August 20, 2012
Published: September 4, 2012

Scheme 1. Schematic Illustration of the Fabrication Process of the Electrochemical AChE Biosensor for AChE Inhibition Assay

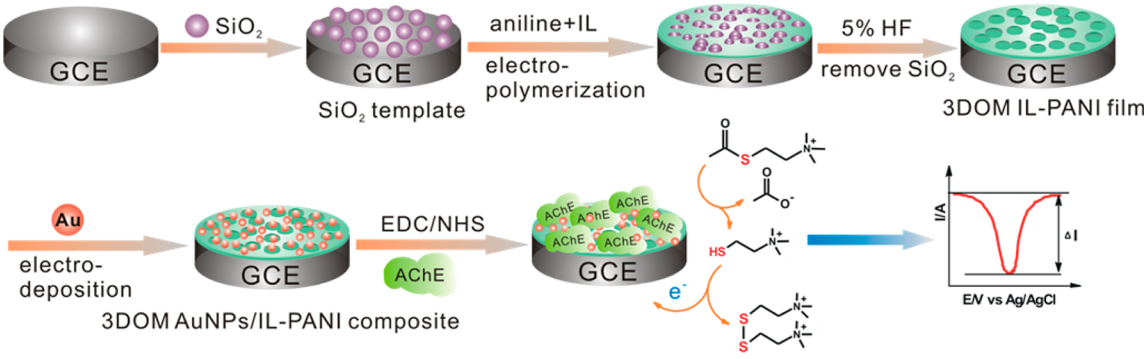

viscosity, and good conductivity. They have been incorporated to conventional materials, such as sol−gel,[34] chitosan,[35] carbon nanotubes,[36] and Nafion[37] for improving conductivity and promoting the electron transfer. Actually, it has been reported that the conductivity of PANI synthesized in ILs was pronouncedly enhanced.[38] Especially, macroporous PANI doped with IL displays highly ordered porous structure and huge surface area. It has successfully been applied in the electrochemical impedance immunoassay of hepatitis B surface antigen.[39]

Acetylcholinesterase (AChE) is a key enzyme in the central nervous system responsible for the termination of impulse signaling at cholinergic brain synapses.[40] The variation of AChE activity plays a critical role in signal transduction of the cholinergic nervous system.[41,42] It has been proved that the inhibition of AChE prevents it from participating in the hydrolysis of acetylcholine (ACh), and thus the cholinergic neurotransmission is disturbed.[43] This is considered to correlate with the pathogenesis of neurodegenerative disorders, such as Parkinson's and Alzheimer's diseases.[44−46] Some researchers have discovered that various chemicals can influence the AChE activity, such as pesticides,[47,48] drugs,[49] and neurotoxins.[50] Among these chemicals, neurotoxins, especially endogenous neurotoxins, have been identified to have great influence on AChE activity.[13] Recently, 1(*R*),2*N*-dimethyl-6,7-dihydroxy-1,2,3,4-tetrahydroisoquinoline (*N*-methyl-(*R*)-salsolinol; (*R*)-NMSal), which is one of the most important endogenous neurotoxins, has been found to result in a concentration-dependent decrease in AChE activity and contribute to the onset and progression of Parkinson's disease (PD) via disrupting the balance between dopamine and ACh.[14] Consequently, exploring rapid and sensitive approaches to evaluate the inhibitory effect of endogenous neurotoxins on AChE activity has biological significance for better understanding the pathogenesis of neurotoxin-induced PD and early clinic diagnosis.

In this work, we present an electrochemical AChE inhibition assay induced by (*R*)-NMSal based on three-dimensional ordered macroporous (3DOM) AuNPs/IL-PANI composite. 3DOM PANI doped with 1-octyl-3-methylimidazolium tetrafluoroborate ([Omim][BF_4]) was first prepared via electropolymerization of aniline in the presence of [Omim][BF_4] using silica nanospheres film as a sacrificial template, and then the silica nanospheres were etched by HF. After that, gold nanoparticles (AuNPs) were electrodeposited on the IL-PANI film to facilitate the electron transfer and thus improve the sensitivity of the biosensor. The prepared composite inherited good electronic conductivity, excellent biocompatibility, and huge porous surface area, which made it an ideal candidate for AChE immobilization. The established electrochemical AChE biosensor exhibited excellent catalytic effect on the hydrolysis of acetylthiocholine chloride (ATCh) and thus was successfully applied to assess the inhibitory effect of (*R*)-NMSal on the AChE activity. Experimental results revealed that (*R*)-NMSal caused a significant decrease in the AChE activity.

EXPERIMENTAL SECTION

Chemicals and Materials. Acetylcholinesterase (AChE) (from *Electrophorus electricus*), acetylthiocholine chloride (ATCh), *N*-methyl-(*R*)-salsolinol [(*R*)-NMSal], 1-ethyl-3-(3-dimethylaminopropyl)carbodiimide (EDC), *N*-hydrosuccinimide (NHS), and aniline were purchased from Sigma Chemicals (St. Louis, MO). The ionic liquid (IL) 1-octyl-3-methylimidazolium tetrafluoroborate ([Omim][BF_4], 99%) was provided by Shanghai Key Laboratory of Green Chemistry and Chemical Processes, East China Normal University (Shanghai, China). Tetraethoxysilane (TEOS) was obtained from Aladdin (Shanghai, China). $HAuCl_4{\cdot}4H_2O$, ammonia solution ($NH_3{\cdot}H_2O$), anhydrous ethanol, and HF were supplied from Shanghai Chemical Reagents Co. Ltd. (Shanghai, China). Phosphate-buffered saline (PBS, 10 mM) containing 136.7 mM NaCl, 2.7 mM KCl, 8.72 mM Na_2HPO_4, and 1.41 mM KH_2PO_4, was adjusted to pH 7.0 and used as the buffer solution. Aniline was distilled under reduced pressure and stored at low temperature prior to use. All of the aqueous solutions were prepared with deionized water from Millipore (Milli-Q, 18.2 MΩ·cm), and all the glasswares were autoclaved prior to use.

Apparatus. All electrochemical measurements were performed with a CHI 660C electrochemical workstation (CH Instruments Inc., Austin, TX) with a conventional three-electrode system comprised of platinum wire as the auxiliary electrode, Ag/AgCl electrode as the reference, and the prepared biosensor as the working electrode. Scanning electron microscopy (SEM) was carried out on an S-4800 (Hitachi Co. Ltd., Tokyo, Japan). Fourier transform infrared (FTIR) spectra were measured on a Nicolet Nexus 670 instrument (Thermo Nicolet Co.). Electrochemical impedance spectroscopy (EIS) was carried out within a frequency range of 10^{-1}−10^5 Hz at an amplitude of 5 mV. All experiments were carried out at room temperature in PBS.

Synthesis of Monodispersed Colloidal SiO_2 Nanospheres. Monodispersed SiO_2 nanospheres were synthesized following the Stöber−Fink−Bohn method:[51] hydrolysis and condensation of TEOS in a mixture of ethanol with water, using ammonia as catalyst to initiate the reaction. Briefly, 7 mL

dx.doi.org/10.1021/jp302792u | *J. Phys. Chem. B* 2012, 116, 11180−11186

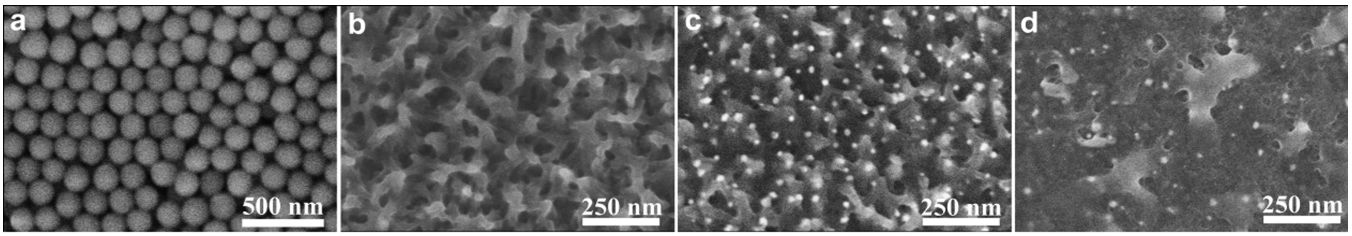

Figure 1. SEM images of (a) SiO_2 colloidal template, (b) IL-PANI/GCE, (c) AuNPs/IL-PANI/GCE, and (d) AChE/AuNPs/IL-PANI/GCE.

of TEOS was dissolved in 100 mL of absolute ethanol, followed by rapid injection of 6 mL of H_2O and 7 mL of $NH_3{\cdot}H_2O$ (25 wt % in H_2O) under vigorous stirring at room temperature. The stirring process was continued for 4 h. Then the nanospheres were separated from the reaction medium by centrifuging at 7000 rpm for 10 min. The precipitate was washed with ethanol and PBS several times and dried in an oven at 60 °C.

Fabrication of AChE Biosensor. The overall procedure for fabrication of AChE biosensor is illustrated in Scheme 1. Prior to surface modification, the GCE (Φ = 3 mm) was polished with 0.05 μm of alumina followed by successive sonication in acetone, HNO_3 (1:1, v/v), NaOH (50%, w/w), and water. SiO_2 nanosphere (0.05 g) was dispersed into 10 mL of water/ethanol (90:10 v/v) mixture by ultrasonication to form the suspension of colloidal SiO_2 nanospheres. Ten microliters of the colloidal suspension was deposited onto the surface of the pretreated GCE and dried under infrared lamp, and then the 3D template was obtained (denoted as SiO_2/GCE).

The GCE with the film of SiO_2 template was submerged into 1.0 M HCl solution containing 0.50 M aniline and 0.04 M [Omim][BF_4], and electropolymerization was carried out by anodic oxidation at a potential of 0.70 V at room temperature for 500 s. During the process, the electropolymerization of aniline occurred on the SiO_2 colloidal crystal template. After polymerization, the resulting film was thoroughly rinsed with 1.0 M HCl and immersed into aqueous HF (5%) for 3 min to remove the SiO_2 nanospheres, and thus the 3DOM IL-PANI film was formed. After that, AuNPs were electrodeposited onto the film via multipotential step from +1.055 to −0.045 V for 15 s in 0.5 M H_2SO_4 containing 0.1 mM $HAuCl_4$,[52] forming AuNPs/IL-PANI composite.

For enzyme immobilization, 10 μL of enzyme solution containing 0.4 M EDC, 0.1 M NHS, and 1.9 mg/mL AChE was dropped on the prepared AuNPs/IL-PANI composite and allowed to dry at room temperature. The fabricated AChE/AuNPs/IL-PANI/GCE was washed thoroughly with distilled water and stored in PBS at 4 °C when not in use.

Inhibition Measurement. The prepared AChE biosensor, acting as the working electrode, was first immersed in 5 mL of PBS containing different concentrations of (*R*)-NMSal. Then the substrate ATCh with a certain concentration was added, and the produced electrochemical signal was recorded with differential pulse voltammetry (DPV) in the range of 0.2−1.0 V with the pulse amplitude of 50 mV and the pulse width of 50 ms.

RESULTS AND DISCUSSIONAN

Characterization of the Modified Electrode. Figure 1 shows the SEM images of SiO_2/GCE, IL-PANI/GCE, AuNPs/IL-PANI/GCE, and AChE/AuNPs/IL-PANI/GCE, respectively. From Figure 1a, we can see that a highly ordered 3D SiO_2 colloidal template is formed on the GCE with a spherical array structure. The prepared SiO_2 are well-dispersed and uniform in size with a diameter of 150 ± 10 nm. When the SiO_2/GCE was subjected to constant potential scanning, aniline could be oxidized and polymerized on the template. The thickness of PANI film was controlled by the reaction time during the electropolymerization process. After a reaction time of 500 s, a dark green film could be observed clearly at the electrode surface, indicating that the polymer has been deposited.[53,54] After the SiO_2 nanospheres were removed by diluted HF solution, the resulting film was characterized by SEM. As shown in Figure 1b, we can see that a good 3DOM IL-PANI film was obtained.

In Figure 1c, it is clearly shown that numerous AuNPs were electrodeposited on the IL-PANI film with diameter ranging from 40 to 50 nm. It is worthy of noting that the AuNPs are distributed not only on the surface but also inside of the IL-PANI film. This uniform and macroporous nanostructure provides an effective electrode surface for enzyme loading and accelerating electron transfer. Figure 1d presents that AChE molecules are well spread on the electrode surface.

The formation of IL-PANI film was also confirmed by FTIR spectra (Figure 2, curve b). As can be seen, the peak at 3450

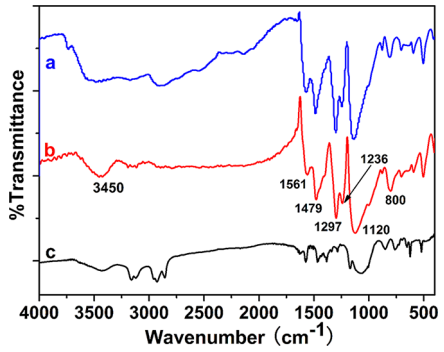

Figure 2. FTIR spectra of (a) PANI, (b) IL-PANI, and (c) IL films.

cm^{-1} is ascribed to the N−H stretching vibrations. The peaks at the 1561 and 1479 cm^{-1} correspond to stretching deformations of the quinoid ring and benzenoid ring, respectively. The strong transmission bands at 1297 and 1120 cm^{-1} are attributed to C−N stretching of the secondary aromatic amine. The peak at 800 cm^{-1} is ascribed to the out-of-plane bending of C−H on the 1,4-disubstituted ring. As for the peak at 1236 cm^{-1}, it is caused by the various stretching and bending associated with C−C bond.[55] The band at 1120 cm^{-1} is assigned to be an electronic-like band, and its intensity is considered to measure the degree of delocalization of electrons on IL-PANI film.[56] Therefore, the high intensity of this peak here proves that the conductivity of IL-PANI is high. This spectrum is found to be similar to that of

dx.doi.org/10.1021/jp302792u | J. Phys. Chem. B 2012, 116, 11180−11186

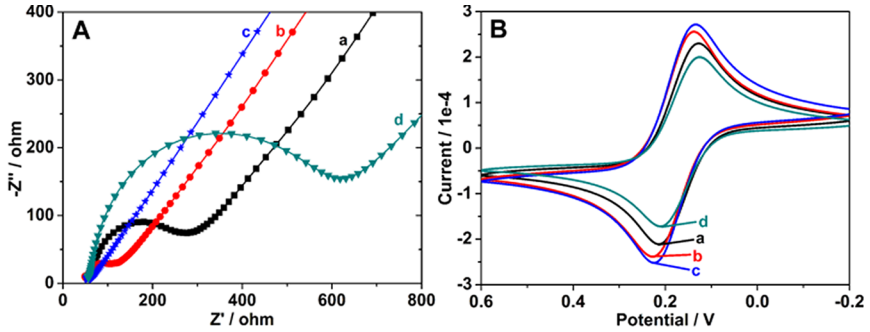

Figure 3. EIS (A) and CV (B) of the electrodes in PBS containing 0.1 M KCl and 2.5 mM $Fe(CN)_6^{3-/4-}$: (a) bare GCE; (b) IL-PANI/GCE; (c) AuNPs/IL-PANI/GCE; (d) AChE/AuNPs/IL-PANI/GCE. The scan rate was 100 mV/s.

PANI film (curve a) and without the obvious characteristic absorption peaks of IL (curve c). It may be due to the small amount of IL during the preparation of IL-PANI film. However, in the spectrum region of 1800−3000 cm^{-1}, the absorbance increases compared to curve a, which can be attributed to the promoted electron transfer due to the presence of IL.[38] This feature suggests that the IL-PANI film can be used as an effective electrode matrix for electrochemical investigation.

Electrochemical Characteristics of the AChE Biosensor. The electrochemical characteristics of the AChE biosensor were studied by EIS and CV, which were performed in PBS containing 0.1 M KCl and 2.5 mM $Fe(CN)_6^{3-/4-}$. EIS, a powerful tool to monitor the features of the electrode surface, confirmed the electrical communication between the redox probe $Fe(CN)_6^{3-/4-}$ and the electrode upon the stepwise modification process (Figure 3A).[57] An electron-transfer resistance (R_{et}) of about 218 Ω is exhibited on bare GCE (curve a). After the IL-PANI film was electropolymerized on the electrode, a lower R_{et} for the redox probe is observed (63 Ω, curve b), indicating that IL-PANIs are excellent electric conducting materials. It is in good agreement with the results from FTIR spectroscopy. When AuNPs were electrodeposited onto the IL-PANI/GCE, we were surprised to observe an almost straight line (curve c). These results indicate that the electron transfer on the AuNPs/IL-PANI/GCE is extremely fast. The immobilization of AChE on the electrode, however, results in great increase in the R_{et} (583 Ω, curve d), suggesting that AChE molecules act as the inert electron and mass-transfer blocking layer and hinder the diffusion of $Fe(CN)_6^{3-/4-}$ toward the electrode surface. This is the direct evidence of successful binding of enzyme on the electrode surface. The number of AChE molecules immobilized on the electrode was estimated to be 3.9×10^{13}, which was determined by AChE ELISA assay kit. CV was further used to study the changes of the electrode behavior after each assembly step, and the results are in correspondence with those from EIS (Figure 3B). EIS and CV results show that the AuNPs/IL-PANI composite could not only act as an effective matrix for AChE loading but also greatly accelerate electron transfer, which would improve the detection sensitivity of the biosensor.

Cyclic Voltammetric Behavior of the AChE Biosensor. Figure 4A displays the typical cyclic voltammograms of different electrodes in the absence and presence of ATCh in PBS. In the absence of ATCh, no redox peak is observed for both bare GCE (curve a) and IL-PANI/GCE (curve b) over the working potential range from 0.2 to 1.0 V. After addition of 0.4 mM ATCh into PBS, an irreversible oxidation peak at 0.64 V is observed on AChE/AuNPs/IL-PANI/GCE (curve d),

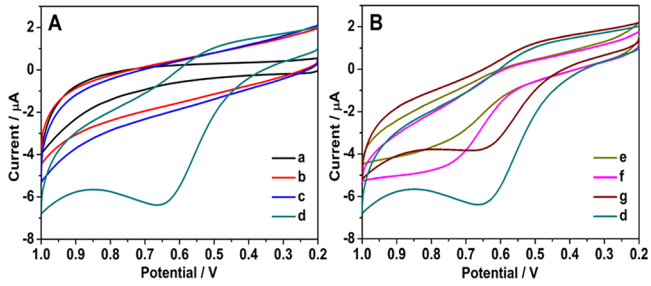

Figure 4. (A) Typical cyclic voltammograms of (a) bare GCE and (b) IL-PANI/GCE in PBS; (c) AuNPs/IL-PANI/GCE and (d) AChE/AuNPs/IL-PANI/GCE in PBS containing 0.4 mM ATCh. (B) Typical cyclic voltammograms of (d) AChE/AuNPs/IL-PANI/GCE, (e) AChE/PANI/GCE, (f) AChE/IL-PANI/GCE, and (g) AChE/AuNPs/PANI/GCE in PBS containing 0.4 mM ATCh. The scan rate was 100 mV/s.

while no detectable signal is seen on AuNPs/IL-PANI/GCE (curve c). Obviously, this peak is attributed to the oxidation of thiocholine, hydrolysis product of ATCh, which is catalyzed by immobilized AChE as follows:[3]

$$\text{acethylthiocholine (ATCh)} + H_2O \xrightarrow[\text{AChE}]{} \text{thiocholine (RSH)} + CH_3COOH$$

$$2\text{RSH(red)} \rightarrow \text{RSSR(ox)} + 2H^+ + 2e^-$$

It demonstrates that AChE could retain its bioactivity when immobilized on AuNPs/IL-PANI composite.

For comparison, the cyclic voltammetric behaviors of ATCh at AChE/PANI/GCE, AChE/IL-PANI/GCE, and AChE/AuNPs/PANI/GCE were also studied. As shown in Figure 4B, the peak current of AChE/IL-PANI/GCE (curve f) and AChE/AuNPs/PANI/GCE (curve g) are 1.8 times and 2.3 times of that of AChE/PANI/GCE (curve e), respectively, and the peak potential of AChE/IL-PANI/GCE (0.74 V) shifts positively compared to that of AChE/AuNPs/PANI/GCE (0.64 V). This phenomenon indicates that IL had the ability to promote the electron transfer, but its inherent conductivity properties and catalytic behaviors are not as good as those of AuNPs. AuNPs play an important role in facilitating the electronic transfer between the enzyme and the electrode surface. Significantly, the AChE/AuNPs/IL-PANI/GCE exhibits four times higher peak current than that of AChE/PANI/GCE. The macroporous structure of the AuNPs/IL-PANI modified 3DOM electrode provides the electrode with high surface area, and the AuNPs/IL-PANI composite displays

dx.doi.org/10.1021/jp302792u | J. Phys. Chem. B 2012, 116, 11180−11186

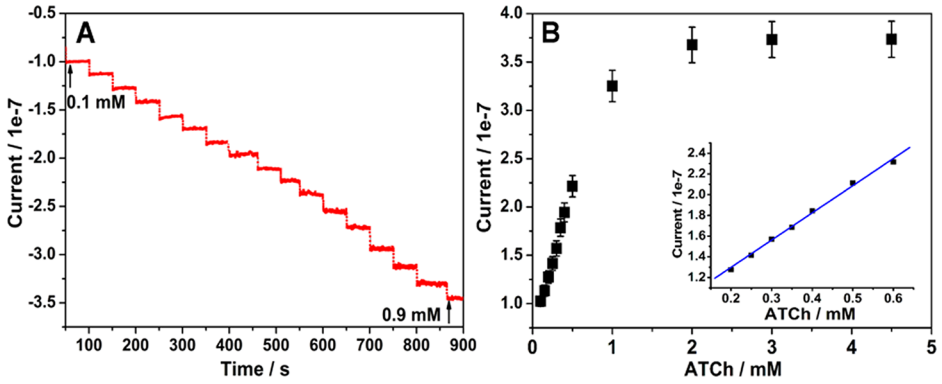

Figure 5. (A) Typical current−time plot for the biosensor on successive addition of ATCh into PBS, with stirring at an applied potential of 0.62 V. (B) Calibration plots for ATCh determination.

combined enhancement effect of good conductivity, which may benefit the electrocatalyzed oxidation of thiocholine.

Dynamic Study of the AChE Biosensor. The AChE biosensor was examined over a range of ATCh concentration from 0 to 5.0 mM in the potentiostatic measurements. Figure 5A depicts the typical amperometric response of the AChE/AuNPs/IL-PANI/GCE polarized at 0.62 V in a stirred solution, to which ATCh stock solution was successively added. It is clear that the biosensor shows a rapid and sensitive response to the change of ATCh concentration, and the response current increases with the increase of ATCh concentration. The corresponding calibration curve is shown in Figure 5B. As expected for the enzymatic catalysis reaction, the response is linear at low substrate concentration from 0.2 to 0.6 mM (inset), but the enzyme becomes saturated at high values of about 2.0 mM. To determine the apparent Michaelis−Menten constant (K'_M), the experimental data were analyzed by the Michaelis−Menten kinetic model. The K'_M of the present AChE biosensor was 0.33 mM calculated from the linear part of the calibration plot using the Lineweaver−Burk equation. This relatively low value is comparable to those previously reported,[58,59] which suggests that the enzyme remains highly functional after immobilization and shows great affinity to its substrate. This is mainly due to the excellent electrotransfer channels of AuNPs/IL-PANI composite.

The repeatability of the proposed AChE biosensor was assessed through repetitively measuring ATCh (0.4 mM) five times. The results indicated that the method possessed a good repeatability with relative standard deviation of 4.2%. The reproducibility was estimated by fabricating four AChE-modified electrodes, and the relative standard deviation was 6.6%. The storage stability of the AChE biosensor was also determined by measuring the change in the current response after a storage period of two weeks. When not used, the AChE biosensor was stored in refrigerator at 4 °C. The biosensor exhibited a quite satisfying stability, which retained 92.3% of its initial response. The long-term stability might be attributed to the high bioactivity and stability of the AChE immobilized on the surface of AuNPs/IL-PANI composite.

Inhibition Measurements. (*R*)-NMSal has been reported to correlate with the development of neurodegenerative disorders. Our study concerning the inhibitory influence of (*R*)-NMSal on AChE activity is of great significance for understanding the pathogenesis of PD. In this work, the AChE/AuNPs/IL-PANI/GCE functioned as an electrochemical biosensor for AChE inhibition measurement with DPV. As shown in Figure 6, a high current response is obtained for the AChE biosensor in the presence of 0.4 mM ATCh (curve a).

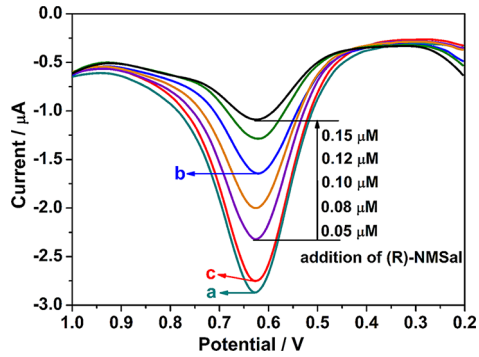

Figure 6. Response of the AChE biosensor in the presence of 0.4 mM ATCh (a) without the inhibitor; (b) with the addition of 0.1 μM (*R*)-NMSal; (c) after exclusion of the inhibitor. Other curves are the responses of the AChE biosensor with increasing concentration of (*R*)-NMSal from 0.05 to 0.15 μM. The scan rate was 100 mV/s.

After the addition of 0.1 μM (*R*)-NMSal, it can be seen that there is a prominent decrease in the peak current (curve b). Furthermore, with increasing concentration of (*R*)-NMSal (from 0.05 to 0.15 μM), there is a corresponding reduction in peak current response. This is attributed to the fact that in the presence of endogenous neurotoxin, the AChE-catalyzed hydrolysis of ATCh is inhibited, which leads to a lower yield of electron donor thiocholine. Obviously, the (*R*)-NMSal-induced AChE inhibition could account for the observed decrease in the peak current. Nevertheless, after the neurotoxin was removed from the electrochemical cell, the initial peak current was almost restored in the presence of 0.4 mM ATCh (curve c). This observation indicates that the endogenous neurotoxin (*R*)-NMSal induces a reversible inhibition of AChE.

To identify the crucial role of AChE inhibition in the decrease of peak current, a control experiment was carried out with huperzine A (HupA), a well-known reversible AChE inhibitor. As observed with that of (*R*)-NMSal, the addition of HupA into the electrochemical cell also caused a considerable decrease in the peak current (data not shown). Furthermore, the removal of HupA allowed restoration of the peak current. These data properly support the proposal that the reversible inhibition of AChE by (*R*)-NMSal is responsible for the reduction of the peak current.

dx.doi.org/10.1021/jp302792u | J. Phys. Chem. B 2012, 116, 11180−11186

CONCLUSIONS

This work has developed an electrochemical AChE biosensor based on 3DOM AuNPs/IL-PANI composite, which possesses good conductivity, highly porous surface area, and good biocompatible properties. The developed AChE biosensor provides a fast and effective approach to the determination of AChE inhibition induced by endogenous neurotoxin. The results demonstrates that the (*R*)-NMSal could lead to concentration-dependent decrease in AChE activity, and the inhibition is reversible. In addition, the AuNPs/IL-PANI composite can also be combined with other enzymes to design electrochemical sensors for the inhibition assay of enzymes.

AUTHOR INFORMATION

Corresponding Author

*E-mail: wzhang@chem.ecnu.edu.cn. Tel.: +86-21-62233509. Fax: +86-21-62232627.

Notes

The authors declare no competing financial interest.

ACKNOWLEDGMENTS

We greatly appreciate the financial support of the National Nature Science Foundation of China (21075041), Science and Technology Commission of Shanghai Municipality (No. 1052 nm06500) and The Research Fund for the Doctoral Program of Higher Education (No.20110076110003).

REFERENCES

(1) Lenigk, R.; Lam, E.; Lai, A.; Wang, H.; Han, Y.; Carlier, P.; Renneberg, R. *Biosens. Bioelectron.* **2000**, *15*, 541−547.
(2) Eltzov, E.; Cosnier, S.; Marks, R. S. *Expert Rev. Mol. Diagn.* **2011**, *11*, 533−546.
(3) Liu, G. D.; Lin, Y. H. *Anal. Chem.* **2006**, *78*, 835−843.
(4) Ghindilis, A. L.; Atanasov, P.; Wilkins, E. *Electroanalysis* **1997**, *9*, 661−674.
(5) Gill, I.; Barazzouk, S. *Trends Biotechnol.* **2000**, *18*, 282−296.
(6) Eng, L. H.; Elmgren, M.; Komlos, P.; Nordling, M.; Lindquist, S. E.; Neujahr, H. Y. *J. Phys. Chem.* **1994**, *98*, 7068−7072.
(7) Chen, C.-C.; Do, J.-S.; Gu, Y. *Sensors* **2009**, *9*, 4635−4648.
(8) Bhattacharyya, M. S.; Hiwale, P.; Piras, M.; Medda, L.; Steri, D.; Piludu, M.; Salis, A.; Monduzzi, M. *J. Phys. Chem. C* **2010**, *114*, 19928−19934.
(9) Hou, S.; Kasner, M. L.; Su, S.; Patel, K.; Cuellari, R. *J. Phys. Chem. C* **2010**, *114*, 14915−14921.
(10) Massad-Ivanir, N.; Shtenberg, G.; Tzur, A.; Krepker, M. A.; Segal, E. *Anal. Chem.* **2011**, *83*, 3282−3289.
(11) Chen, D.; Wang, G.; Li, J. *J. Phys. Chem. C* **2007**, *111*, 2351−2367.
(12) Schwartzberg, A. M.; Zhang, J. Z. *J. Phys. Chem. C* **2008**, *112*, 10323−10337.
(13) Wang, Y.; Shao, Y.; Matson, D. W.; Li, J.; Lin, Y. *ACS Nano* **2010**, *4*, 1790−1798.
(14) Zhu, W.; An, Y.; Luo, X.; Wang, F.; Zheng, J.; Tang, L.; Wang, Q.; Zhang, Z.; Zhang, W.; Jin, L. *Chem. Commun.* **2009**, 2682−2684.
(15) Zhu, W.; Wang, D.; Zheng, J.; An, Y.; Wang, Q.; Zhang, W.; Jin, L.; Gao, H.; Lin, L. *Clin. Chem.* **2008**, *54*, 705−712.
(16) Liu, J.; Lu, Y. *J. Am. Chem. Soc.* **2003**, *125*, 6642−6643.
(17) Matsuura, H.; Sato, Y.; Niwa, O.; Mizutani, F. *Anal. Chem.* **2005**, *77*, 4235−4240.
(18) Geng, J.; Liang, J.; Wang, Y.; Gurzadyan, G. G.; Liu, B. *J. Phys. Chem. B* **2011**, *115*, 3281−3288.
(19) El-Sayed, I. H.; Huang, X.; El-Sayed, M. A. *Nano Lett.* **2005**, *5*, 829−834.
(20) Gerard, M.; Chaubey, A.; Malhotra, B. D. *Biosens. Bioelectron.* **2002**, *17*, 345−359.
(21) Gamby, J.; Lazerges, M.; Girault, H. H.; Deslouis, C.; Gabrielli, C.; Perrot, H.; Tribollet, B. *Anal. Chem.* **2008**, *80*, 8900−8907.
(22) Virji, S.; Kaner, R. B.; Weiller, B. H. *J. Phys. Chem. B* **2006**, *110*, 22266−22270.
(23) Diaz, A. F.; Logan, J. A. *J. Electroanal. Chem.* **1980**, *111*, 111−114.
(24) Mu, S. *J. Phys. Chem. B* **2008**, *112*, 6344−6349.
(25) Raitman, O. A.; Katz, E.; Bückmann, A. F.; Willner, I. *J. Am. Chem. Soc.* **2002**, *124*, 6487−6496.
(26) Tian, S. J.; Armstrong, N. R.; Knoll, W. *Langmuir* **2005**, *21*, 4656−4660.
(27) Sun, P.; Armstrong, D. W. *Anal. Chim. Acta* **2010**, *661*, 1−16.
(28) Wei, D.; Ivaska, A. *Anal. Chim. Acta* **2008**, *607*, 126−135.
(29) Lu, X.; Zhang, Q.; Zhang, L.; Li, J. *Electrochem. Commun.* **2006**, *8*, 874−878.
(30) Antonietti, M.; Kuang, D.; Smarsly, B.; Zhou, Y. *Angew. Chem., Int. Ed.* **2004**, *43*, 4988−4992.
(31) Maleki, N.; Safavi, A.; Tajabadi, F. *Anal. Chem.* **2006**, *78*, 3820−3826.
(32) Innis, P. C.; Mazurkiewicz, J.; Nguyen, T.; Wallace, G. G.; MacFarlane, D. *Curr. Appl. Phys.* **2004**, *4*, 389−393.
(33) Liu, H.; Liu, Y.; Li, J. *Phys. Chem. Chem. Phys.* **2010**, *12*, 1685−1697.
(34) Liu, Y.; Wang, M.; Li, J.; Li, Z.; He, P.; Liu, H.; Li, J. *Chem. Commun.* **2005**, 1778−1780.
(35) Lu, X. B.; Hu, J. Q.; Yao, X.; Wang, Z. P.; Li, J. H. *Biomacromolecules* **2006**, *7*, 975−980.
(36) Liu, Y.; Huang, L.; Dong, S. *Biosens. Bioelectron.* **2007**, *23*, 35−41.
(37) Chen, H. J.; Wang, Y. L.; Liu, Y.; Wang, Y. Z.; Qi, L.; Dong, S. J. *Electrochem. Commun.* **2007**, *9*, 469−474.
(38) Wei, D.; Kvarnström, C.; Lindfors, T.; Ivaska, A. *Electrochem. Commun.* **2006**, *8*, 1563−1566.
(39) Li, X. H.; Dai, L.; Liu, Y.; Chen, X. J.; Yan, W.; Jiang, L. P.; Zhu, J. J. *Adv. Funct. Mater.* **2009**, *19*, 3120−3128.
(40) Schumacher, M.; Camp, S.; Maulet, Y.; Newton, M.; MacPhee-Quigley, K.; Taylor, S.; Friedmann, T.; Taylor, P. *Nature* **1986**, *319*, 407−409.
(41) Mesulam, M. *Learn. Mem.* **2004**, *11*, 43−49.
(42) Calabresi, P.; Picconi, B.; Parnetti, L.; Filippo, M. D. *Lancet Neurol.* **2006**, *5*, 974−983.
(43) Lotti, M. *Clin. Chem.* **1995**, *41*, 1814−1818.
(44) Ohno, K.; Engel, A. G.; Brengman, J. M.; Shen, X. M.; Heidenreich, F.; Vincent, A.; Milone, M.; Tan, E.; Demirci, M.; Walsh, P.; Nakano, S.; Akiguchi, I. *Ann. Neurol.* **2000**, *47*, 162−170.
(45) Ceravolo, R.; Volterrani, D.; Frosini, D.; Bernardini, S.; Rossi, C.; Logi, C.; Manca, G.; Kiferle, L.; Mariani, G.; Murri, L.; Bonuccelli, U. *J. Neural Transm.* **2006**, *113*, 1787−1790.
(46) Takada-Takatori, Y.; Kume, T.; Sugimoto, M.; Katsuki, H.; Sugimoto, H.; Akaike, A. *Neuropharmacology* **2006**, *51*, 474−486.
(47) Du, D.; Ye, X.; Cai, J.; Liu, J.; Zhang, A. *Biosens. Bioelectron.* **2010**, *25*, 2503−2508.
(48) Wang, Y.; Zhang, S.; Du, D.; Shao, Y.; Li, Z.; Wang, J.; Engelhard, M. H.; Li, J.; Lin, Y. *J. Mater. Chem.* **2011**, *21*, 5319−5325.
(49) Tan, E. V.; Lowe, C. R. *Anal. Chem.* **2009**, *81*, 7579−7589.
(50) Hossain, S. M. Z.; Luckham, R. E.; Smith, A. M.; Lebert, J. M.; Davies, L. M.; Pelton, R.; Filipe, C. D. M.; Brennan, J. D. *Anal. Chem.* **2009**, *81*, 5474−5483.
(51) Stöber, W.; Fink, A.; Bohn, E. *J. Colloid Interface Sci.* **1968**, *26*, 62−69.
(52) Dai, X.; Nekrassova, O.; Hyde, M. E.; Compton, R. G. *Anal. Chem.* **2004**, *76*, 5924−5929.
(53) Zhao, M.; Wu, X.; Cai, C. *J. Phys. Chem. C* **2009**, *113*, 4987−4996.
(54) Deepa, M.; Ahmad, S.; Sood, K. N.; Alam, J.; Ahmad, S.; Srivastava, A. K. *Electrochim. Acta* **2007**, *52*, 7453−7463.
(55) Kan, J. Q.; Lv, R.; Zhang, S. *Synth. Met.* **2004**, *145*, 37−42.
(56) Wang, Z.; Liu, S.; Wu, P.; Cai, C. *Anal. Chem.* **2009**, *81*, 1638−1645.

(57) Cui, R.; Huang, H.; Yin, Z.; Gao, D.; Zhu, J. *Biosens. Bioelectron.* **2008**, *23*, 1666−1673.
(58) Du, D.; Chen, S. Z.; Cai, J.; Song, D. D. *J. Electroanal. Chem.* **2007**, *611*, 60−66.
(59) Joshi, K. A.; Tang, J.; Haddon, R.; Wang, J.; Chen, W.; Mulchandani, A. *Electroanalysis* **2005**, *17*, 54−58.